Performances of Large-Diameter Cast-in-Place Concrete Pipe Piles and Pile Groups under Lateral Loads

Han-Long Liu[1]; Gang-Qiang Kong, Aff.M.ASCE[2]; Xuan-Ming Ding[3]; and Yu-Min Chen[4]

Abstract: Large-diameter cast-in-place concrete pipe (PCC) pile is widely used for pile foundation and pile-supported embankment over soft clay in China. However, studies on PCC pile-soil reactions (*p-y* curves) or performance of the pile groups under lateral load are not widely reported. A large-scale model test of a single PCC pile under lateral load is carried out, and its lateral bearing capacity, bending moment, and *p-y* curves are measured and analyzed. The deflection and bending moment of this PCC pile is calculated by the *p-y* curves method and modified pile modulus using *LPILE* software. Three-dimensional numerical analyses are conducted using *ABAQUS* software. The reliability and accuracy of the numerical simulation model are verified by comparing the results of the large-scale model test with the *LPILE* calculation. The distribution of deflection and bending moment along the pile and pile group efficiencies of the PCC piles are comparatively analyzed with those of a drilled shaft, which has the same concrete volume. Then, the lateral performance of the PCC pile-supported embankment influence factors are analyzed and discussed. The results show that the PCC piles under lateral load can be calculated by the *p-y* curves developed for drilled shaft and modified pile modulus using *LPILE* software. It also shows that PCC pile-supported embankment is more cost effective than conventional pile (solid circular section pile) supported embankment. **DOI: 10.1061/(ASCE)CF.1943-5509.0000304.**

CE Database subject headings: Embankments; Pipe piles; Lateral loads; Model tests; Numerical analysis; Deflection; Bending.

Author keywords: Embankment; Place concrete pipe (PCC) pile; Lateral load; Large-scale model test; Numerical analysis; Deflection; Bending moment.

Introduction

Many highways, seaports, and high-speed railways are constructed over soft clay in China. Large postconstruction settlement and low bearing capacity are two major problems that exist in engineering practice. Pile-supported embankment is one of the effective and economic solutions used for soft ground treatment. When compared with other traditional soft soil improvement methods, pile-supported embankment has many advantages, such as small lateral deformation, rapid construction, and easily controlled settlements. Pile-supported embankments are widely used in the world, for example, a railway widening project at Stansted Airport in London using pile-supported embankment was reported by Jones et al. (1990). The use of mixed soil and cement columns in an embankment to reduce the differential settlements of a bridge's approaches was illustrated by Lin and Wong (1999). Vibroconcrete columns and geogrids used for widening an existing roadway were reported by Han and Akins (2002). Based on the performance investigation of 13 pile-supported and geogrid-reinforced earth platforms, Han and Gabr (2002) recommended that area ratio could be reduced to 10–20%, in comparison with the relatively high area ratio of only pile-supported embankments (50–70%). Two cases of different pile-supported embankment type over soft ground in China were reported by Chen et al. (2010).

Large lateral loads (e.g., horizontal force caused by a train brake, wave loading, lateral load caused by an earthquake) exist in engineering. In a pile-supported embankment system, the horizontal forces caused by embankment soil slope and train brake should be considered. Large-diameter, cast-in-place concrete pipe (PCC) (tubular) piles (China Patent Nos. ZL02112538.4 and ZL01113719.3, U.S. Patent No. 6749372 B2) are widely used for embankment over soft ground in China. One PCC pile-supported embankment case study shows that only an 8.7% area ratio was used for highway soft ground treatment (Liu et al. 2007). The PCC pile driving effects were studied by Xu et al. (2006) and Liu et al. (2009). Lateral field static load tests were carried out in the Hang-Qian Highway embankment site by Ma et al. (2006), and at the Xuyang Road embankment site by Zhu et al. (2006). The lateral load versus pile top deflection and lateral soil pressures along the pile shaft were measured and analyzed. However, the *p-y* curves for the PCC piles have not been reported in these studies. Based on small-scale model tests, PCC piles with different lengths and outer diameters embedded in sand under lateral loads were reported by Ma et al. (2006). The observations of load versus deflection curves, bending moment, and lateral soil pressures along the pile shaft were presented.

The *p-y* curve method (American Petroleum Institute 1993), which describes nonlinear lateral interaction between soils and piles, is a useful method for lateral bearing capacity calculations. The *p-y* criteria, together with numerical programs, such as *COM624P*

[1]Professor, Key Laboratory for Ministry of Education for Geomechanics and Embankment Engineering, College of Civil and Transportation Engineering, Hohai Univ., Xikang Rd., No.1, Nanjing, Jiangsu 210098, P.R. China (corresponding author). E-mail: hliuhhu@163.com

[2]Associate Professor, College of Civil and Transportation Engineering, Hohai Univ., Xikang Rd., No.1, Nanjing, Jiangsu 210098, P.R. China. E-mail: gqkong1@163.com

[3]Associate Professor, National Engineering Research Center of Water Resources Efficient Utilization and Engineering Safety, Hohai Univ., Xikang Rd., No.1, Nanjing, Jiangsu 210098, P.R. China. E-mail: dxmhhu@163.com

[4]Associate Professor, College of Civil and Transportation Engineering, Hohai Univ., Xikang Rd., No.1, Nanjing, Jiangsu 210098, P.R. China. E-mail: ymchenhhu@163.com

Note. This manuscript was submitted on March 15, 2011; approved on October 17, 2011; published online on October 20, 2011. Discussion period open until September 1, 2013; separate discussions must be submitted for individual papers. This paper is part of the ***Journal of Performance of Constructed Facilities***, Vol. 27, No. 2, April 1, 2013. ©ASCE, ISSN 0887-3828/2013/2-191–202/$25.00.

(Wang and Reese 1993) or *LPILE* (Reese et al. 2004), provide a useful framework for modeling the nonlinear lateral interaction between soils and piles. Until now, there have been no *p-y* curves or criteria developed for the PCC pile. It is necessary to find suitable *p-y* curves and criteria for the PCC pile. Therefore, the *p-y* curves of the PCC pile should be measured through large-scale model tests or field tests. It is evident from the literature cited that most of the research has focused on ultimate lateral bearing capacity of a single PCC pile, while there is little study of PCC pile-soil reactions (*p-y* curves) or the performance of PCC pile or pile groups compared with that of drilled shafts under lateral load. Hence, a large-scale model test of the PCC pile under lateral load is presented here, and its lateral bearing capacity, bending moment, and *p-y* curves are obtained. Three-dimensional (3D) numerical analyses are conducted using *ABAQUS* software. The reliability and accuracy of the numerical simulation model is verified by comparing the results of the large-scale model test with the *LPILE* calculations. A drilled shaft with the same concrete volume is built for comparative analysis. The distribution of the deflection and bending moment along the pile, and the pile group efficiencies of the PCC piles, are comparatively analyzed. Then, the lateral performance of the PCC pile-supported embankment influenced by vertical loads, cushion thickness, and replacement rate are analyzed and discussed.

Large-Scale Model Test

Model Test Equipment

The large-scale model test facility is comprised of a fairly rigid model container, loading system, and measuring system. A view of the large-scale model test facility is shown in Fig. 1. The model container's size is $5 \times 4 \times 7$ m ($16.404 \times 13.123 \times 22.966$ ft) (length $\times$ width $\times$ height). The loading system consists of hydraulic jacks, a hydraulic pressure pump, and a reaction wall. The measuring system consists of load cells, steel bar meters, earth pressure cells, a frequency instrument, LVDTs, and a data acquisition system. The test components' layout and sizes are shown in Fig. 2. During the loading tests, one specific lateral load is set, and then the corresponding deflection is predicted. The load and deflection values are measured by load cells and LVDTs, respectively. The pile side stress distribution along the pile is measured by the reinforcement stress meter embedded in the concrete; the soil pressure distribution along the pile is measured by the earth pressure cells embedded in the soils. Data from the load cells, the reinforcement stress meter, earth pressure cells, and the LVDTs are captured by a data acquisition system. The bending moments of the PCC pile along the pile are calculated by the pile side stresses and its distances; the pile head rotation angle is calculated by two measured deflection differences through two LVDTs placed on the pile head. Assuming the PCC pile is under rigid rotation, the lateral deflections along the pile are calculated through pile head rotation angle and deflection. The soil pressure sensors are placed close to the pile-soil interface. The distance between the pile side and the soil pressure sensors is approximately 10 mm (0.394 in.).

Model Pile and Soils

The instruments' layout is shown in Fig. 2. The PCC pile model with 6-m (19.685-ft) length L, 1.0-m (3.281-ft) outer diameter D_{out}, and 0.12-m (0.394-ft) wall thickness t is cast with C20 concrete and a reinforcement cage. The reinforcement cage is composed of 8Φ16 primary steel, Φ6 at 250 stirrups in the bottom 5-m length, and Φ6 at 100 stirrups in the top 1-m (3.281-ft) length. To avoid stress concentration on the circular pile head under the lateral load, saddle-shaped PCC pile top, where the lateral load is applied, is shown in Fig. 1. Twenty-six steel stress meters are symmetrically arranged on the two symmetrical primary steel bars; 16 earth pressure cells are symmetrically embedded in the pile surrounding the soil along the pile.

Both clay and sand, which were filled into the model container, are taken from the Hexi District of Nanjing, China. The top soil layer is clay with 3.5-m (11.483-ft) depth; the bottom layer is sand with 3.2-m (10.499-ft) depth. The sand is uniformly graded. Its uniformity coefficient (C_u) and curvature coefficient (C_c) are 1.58 and 0.99, respectively. The soil layers are filled in the container by controlling the density of the in-place dry soils. Soil layers in the model container are filled and compacted artificially, and the soil density is checked by sampling tests. In order to keep the moisture content of backfilled clay, water was pulled on clay layer surface each day during the finished backfill and testing time. Hence, the groundwater table is nearly on the top of the clay layer. The physical and mechanical indices of soils with the specified density are shown in Table 1, which are determined by laboratory tests. The results of the cone penetration tests for the model soils are shown in Fig. 3.

Model Test Standard

A one-way multicycle loading method is used in this model's test work. Nine steps with 20 kN (4.496 kips) for each load grade (total

Fig. 1. Diagram of large-scale model test facility

J. Perform. Constr. Facil. 2013.27:191-202.

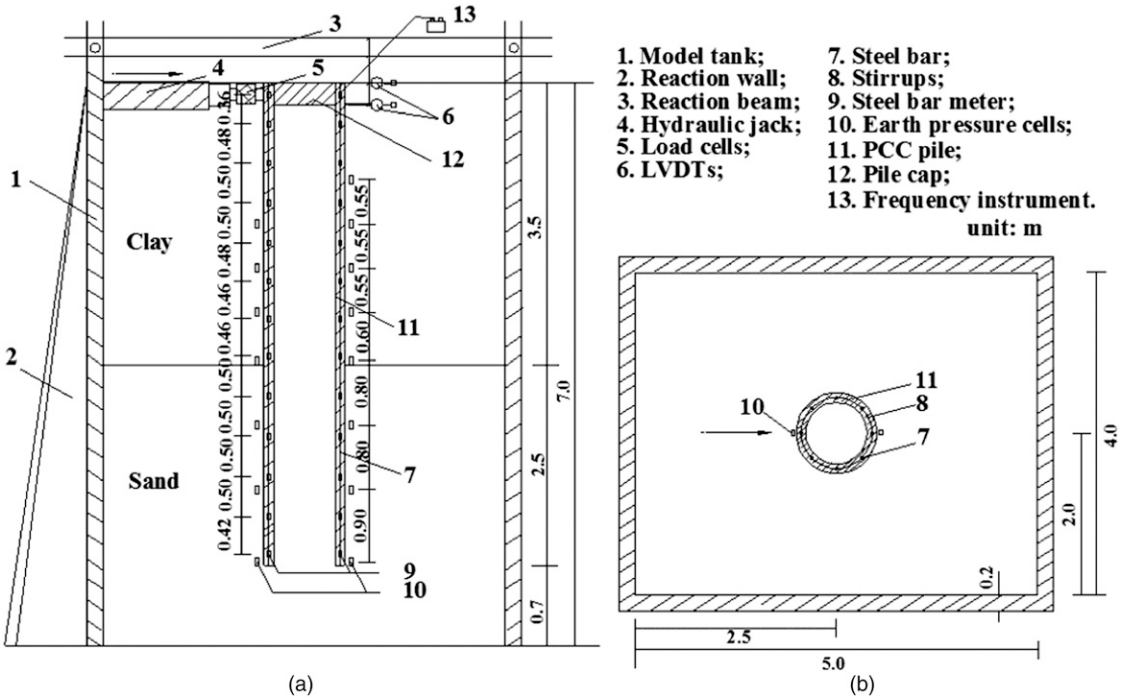

Fig. 2. Schematic diagrams of the experimental setup under the lateral load: (a) vertical profile; (b) horizontal profile

Table 1. Physical and Mechanical Parameter Indices of Soils with Specified Density Used in Model Test, *LPILE*, and *ABAQUS* Verification Models

Materials	Clay	Sand
Proportion, G_s	2.70	2.65
Void ratio, e_0	0.84	—
Natural moisture content, ω (percentage)	30.10	6.63
Maximum dry density, ρ_{max} (g/cm^3)	—	1.64
Minimum dry density, ρ_{min} (g/cm^3)	—	1.35
Natural unit weight, γ (kN/m^3)	18.72	15.58
Depth, z (m)	3.50	2.50
Cohesion, c_{cu} (kPa)	24.00	15.00
Friction angle, φ_{cu} (°)	27.00	38.00
Compression modulus, E_s (MPa)	4.60	17.00
Moisture content, ω (percentage)	16.70	5.00
Control unit weight, γ (kN/m^3)	14.70	15.19

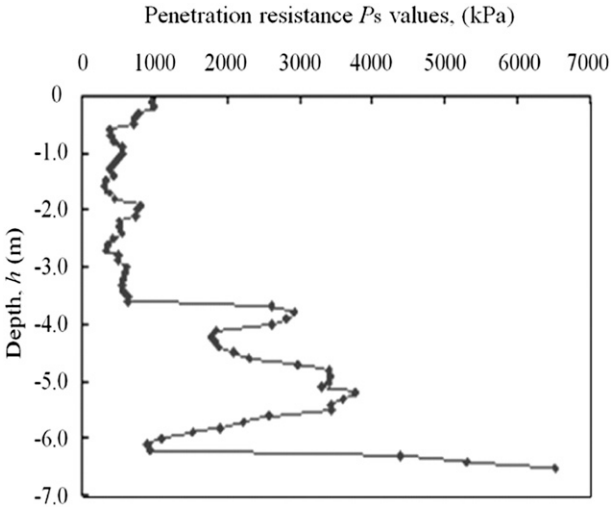

Fig. 3. Cone penetration tests results for model test soils site conditions

load = 180 kN [40.464 kips]) are carried out. For each step, keeping each specific loading 4 min, the deflections, steel bar meter, and soil pressures are observed and recorded; then after unloading, the residual deflections after 2 min are recorded; one cycle has been finished. Five cycle times are taken for each load. According to JGJ94-2008 (2008), termination of loading is based on the following criteria: (1) pile bodies fracture; (2) the deflections of the pile top being larger than 30 mm (1.181 in.); (3) the maximum loading ability or maximum deflections is reached; or (4) the deflections rapidly increase under constant loading. When the test condition reaches any of these criteria, the test should be stopped.

Model Test Results and Discussions

The curve of the cycle lateral load and deflection (H_0-y_0 curve) is shown in Fig. 4(a). It shows that the deflections increase with increasing lateral load. When the lateral load is under 80 kN (17.984 kips), deflection increases nearly linearly. When the lateral load reaches 120 kN (26.976 kips), the deflection increases rapidly and an observable crack develops in the surrounding soils. When the lateral load reaches 160 kN (35.968 kips), the deflection is 31.82 mm (1.253 in.). Then, the model test loading is stopped. Figs. 4(b and c) show the pile head lateral load versus the deflection gradient ($H_0 - \Delta y_0/\Delta H_0$ curve), and the pile head lateral load versus the stress in the maximum bending moment, respectively. Based on JGJ94-2008 (2008), the critical lateral load capacity and the ultimate lateral load capacity of the PCC pile are 80 kN (17.984 kips) and 120 kN (26.976 kips), respectively. The corresponding deflections are equal to 2.59 (0.102 in.) and 9.16 mm (0.361 in.), respectively.

Fig. 5 shows the distribution of the bending moment of the PCC pile along the pile, where the maximum value of the bending

J. Perform. Constr. Facil. 2013.27:191-202.

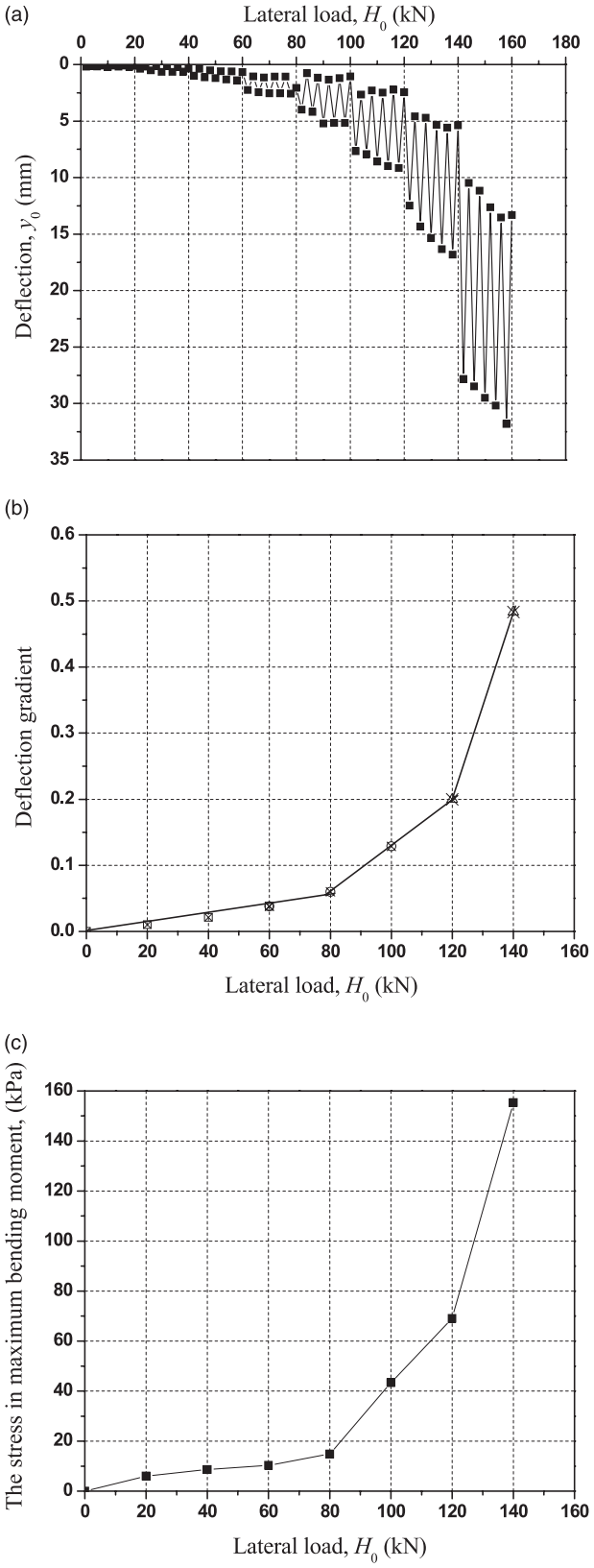

Fig. 4. Curves of the lateral load versus the deflection for the PCC pile: (a) $H_0 - y_0$ curves; (b) load versus deflection gradient curve; and (c) load versus stress of maximum bending moment

moment occurs approximately 2.5 m (8.202 ft) below the pile head. Model tests indicate that small cracks occur 2.2–2.5 m (7.218–8.202 ft) below the pile head. The bending moments increase in the range of 0 to −2.5 m (0 to −8.202 ft) and then decrease along the pile under the specified load. The bending moments increase with increasing pile head lateral load.

Fig. 6 shows the *p-y* curves for the PCC pile-clay and PCC pile-sand, obtained by this large-scale model test. Net soil resistance per unit shaft length p and corresponding deflection of the pile y are measured or calculated by earth pressure cells and LVDTs, respectively. The length of the model pile is 6 m (19.685 ft), and therefore it is assumed that the pile is under rigid rotation. Using the top two LVDTs, the pile head deflections and rotation angles under each lateral load can be measured. The deflections along the pile can be calculated through pile head deflections and rotation angles. The characteristics of the *p-y* curves of the PCC pile are similar to those of a conventional drilled shaft (Reese et al. 2004).

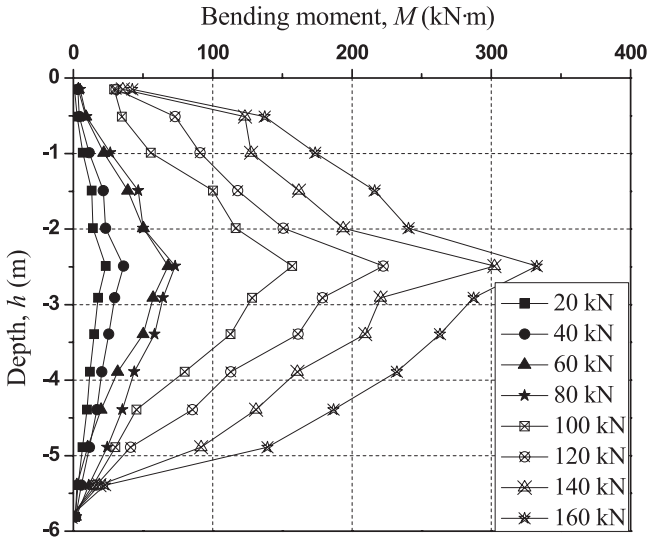

Fig. 5. Distributions of bending moments along the PCC pile depth under different lateral loads

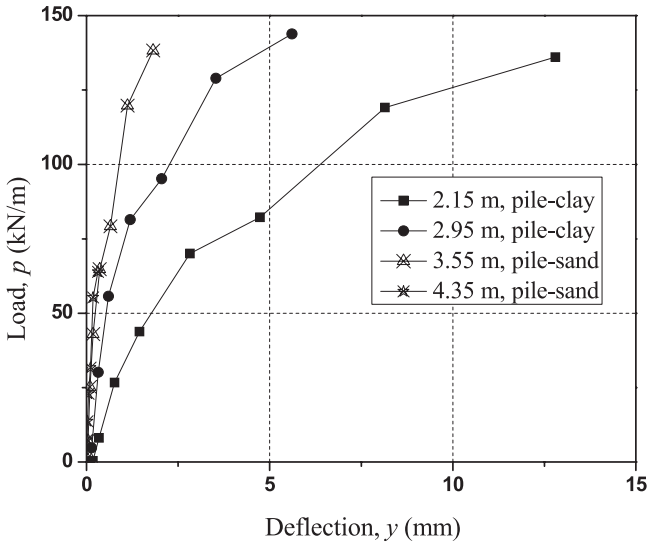

Fig. 6. Curves of the lateral load versus the deflection at different PCC pile depths (p-y curves)

J. Perform. Constr. Facil. 2013.27:191-202.

Numerical Analyses

Numerical Model Built and Parameter Selection

Vertical and horizontal profiles of the PCC pile-supported embankment system used in the numerical simulation are shown in Fig. 7. Fig. 7(a) shows the embankment, cushion layer, which is mixed with crushed rock and geogrid, and PCC piles with or without a pile cap. Fig. 7(b) shows different pile arrangements, pile diameters, pile spacing, and a pile cap of the PCC piles. The embankment vertical loads and lateral loads are simplified as a uniform load acting on the cushion layer. PCC piles are embedded in soft soils with 15-m (49.213-ft) length L, 1.0-m (3.280-ft) outer diameter D_{out}, and 0.12-m (0.394-ft) wall thickness t. Conventional drilled shaft models with 15-m (49.213-ft) length L and 0.65-m (2.133-ft) diameter D_0, which have the same concrete volume as that of the PCC pile, are also built for comparative analysis. Owing to symmetry, only a quarter of the whole meshes were used in the 3D simulation. The geometric model and typical finite-element meshes for the 3×3 pile group without the pile cap are shown in Fig. 8. In the simulation, the pile is modeled as an isotropic elastic linear model; soils are modeled as a Mohr-Coulomb model. The interfaces of the pile-soils (contained soil inside the pile and the soil outside the pile) are modeled as a Coulomb sliding model, in which the friction coefficient of the pile-soil interface is assumed to be that of the soils. The upper boundary condition is assumed as a free boundary; the side boundary condition is assumed to be a level-direction sliding support; and the bottom boundary condition is assumed to be a vertical-direction sliding support. The groundwater table is assumed to be at the ground surface. Conventional soil profiles and pile parameters used for influence factors analysis in the numerical simulation are shown in Table 2. The soil profiles shown in Table 2, are different with those of model test, *LPILE*, and verification numerical model.

Verification

To verify the numerical simulation model, the comparative analysis is built based on the model test condition. The soil properties (Table 1) and pile parameters are the same, as measured by the model test. At the same time, another calculation based on the *p-y* curves method model is built using *LPILE* software for comparative analysis. The *p-y* curves of soft clay (Matlock 1970) and sand (Reese et al. 1974) are used for modeling clay and sand. The modified PCC pile modulus, whose value is obtained by the modulus of the pile multiplied by the cross-section area of the pipe pile plus the modulus of the soils multiplied by the cross-section area of the pile core soils, then divided by the total areas of the pipe pile and the pile core soils, is used in the *LPILE* calculation. The input data of the soil properties for the *LPILE* software analysis are shown in Table 3.

Fig. 9 shows the comparison curves of the numerical simulation pile head lateral load versus the deflection of the *LPILE* calculation and model test results. Fig. 9 shows that the H_0-y_0 curves are slow variant. Based on JGJ94-2008 (2008), one of the ultimate lateral bearing capacity decided methods for the H_0-y_0 curve is the bilinear method. The bearing capacity value is the intersection of two lines. One line is the tangent of the zero point on curve, the other line is the tangent of the curve where deflection equals 30 mm. Hence, the ultimate lateral bearing capacity obtained by the model test, numerical simulation, and the *LPILE* calculation are 120.0 kN (26.976 kips), 125.5 kN (28.212 kips), and 115.0 kN (25.852 kips), respectively, in which the simulation error is less than 5.0%. Fig. 10 shows the comparison curves of the numerical simulation and the *LPILE* calculation bending moment distributions along the pile under different loads with those of the model test results. The numerical simulation bending moment results and the *LPILE* calculated results fit well with those of the model test results. The single PCC pile numerical simulation model is verified by the model test results. The same method was used to build the PCC pile groups and the PCC pile-supported embankment under lateral load numerical simulation models. The analysis of influence factors results obtained from the pile groups or the pile-supported embankment are also reliable and accurate.

Numerical Simulation Conditions

To compare the lateral performances of the PCC pile and the drilled shaft under different conditions, numerical simulations are conducted. Three types, with or without cushion layer, with or without a pile cap, and different pile spacing ($2D_0$–$16D_0$, where D_0 is the diameter of circular pile), are studied. To analyze the performance of the PCC pile-supported embankment, the influence factors analysis, such as vertical load grades, cushion thickness, concrete replacement rate, and pile numbers, is taken. The comparative analysis conditions of the cushion layer, pile cap, and pile spacing are shown in Table 4. The influence factors analysis conditions are shown in Table 5.

Comparative Analysis between Cast-in-Place Concrete Pipe Pile and Drilled Shaft

Influence Analysis with/without Cushion Layer

The comparative analysis was based on a single pile without a pile cap. For piles under lateral load directly (without cushion layer), the distributions of the deflection and bending moment along the pile for the PCC pile and drilled shaft under 200-kN (44.960-kips) lateral load are shown in Fig. 11. Fig. 11(a) shows that the changes of the deflection for the PCC pile and the drilled shaft occur 6–7 m (19.685–22.966 ft) below the pile top. The maximum values are developed at the pile top, and are 8.8 mm (0.346 in.) and 27.1 mm (1.067 in.), respectively. This means that the lateral bearing capacity of the PCC pile can be improved nearly 2.1 times compared with that of a drilled shaft with the same concrete volume. Fig. 11(b) shows that the distribution of the bending moments along the PCC pile is similar to that of the drilled shaft, and the values are larger than those of the drilled shaft. Both maximum values of the bending moment are developed at 3 m (9.843 ft) below the pile top, and are 276.4 kN·m (203.873 ft·kips) and 251.6 kN·m (185.580 ft·kips), respectively. The results show that the maximum deflections of a PCC pile are decreased nearly 70% compared with those of the drilled shaft, while the maximum bending moments of the PCC pile are improved nearly 10% compared with those of the drilled shaft.

For piles under vertical and lateral load through the cushion soil layer (with cushion layer), the distribution of the deflection and bending moment along the pile for the PCC pile and drilled shaft under 125-kPa (18.142-psi) lateral load and 100-kPa (14.514-psi) uniform vertical load are shown in Fig. 12. Fig. 12(a) shows that the distribution of the deflections along the pile of the PCC pile is similar to that of the drilled shaft, and the values are larger than those for the drilled shaft. Fig. 12(b) shows that the distribution of the bending moments along the pile of the PCC pile is larger than that of the drilled shaft, and the maximum value is nearly 3.0 times that of the drilled shaft. Both the maximum values of the bending moment are developed at 4 m (13.123 ft) below the pile top, and are 71.0 kN·m (52.370 ft·kips) and 24.4 kN·m (17.997 ft·kips), respectively. The PCC pile has a larger diameter than that of the drilled shaft, which causes the gross section areas of the PCC pile to be nearly 2.4 times

J. Perform. Constr. Facil. 2013.27:191-202.

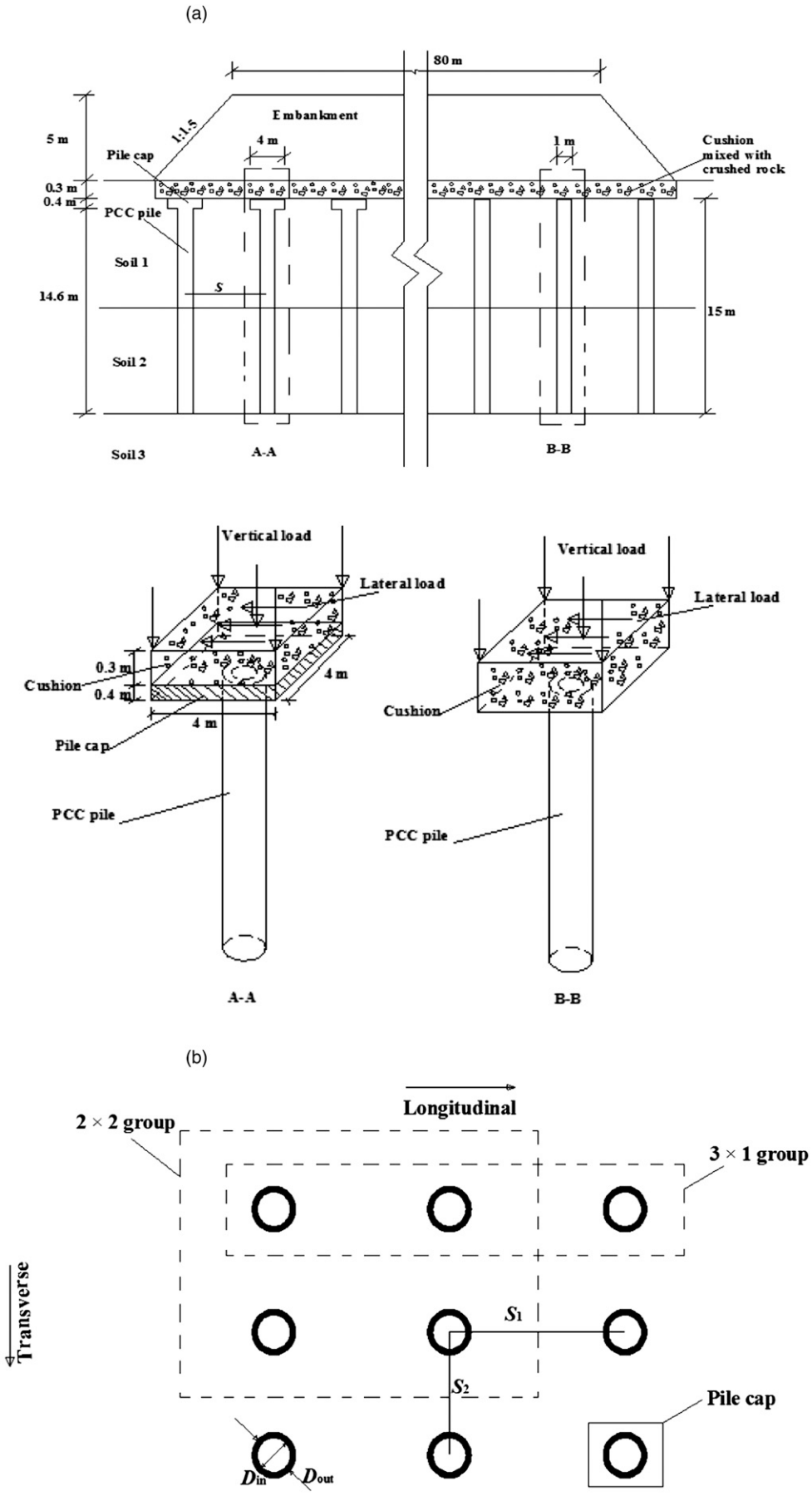

Fig. 7. Schematic diagrams of numerical simulation models: (a) vertical profile; (b) horizontal profile

J. Perform. Constr. Facil. 2013.27:191-202.

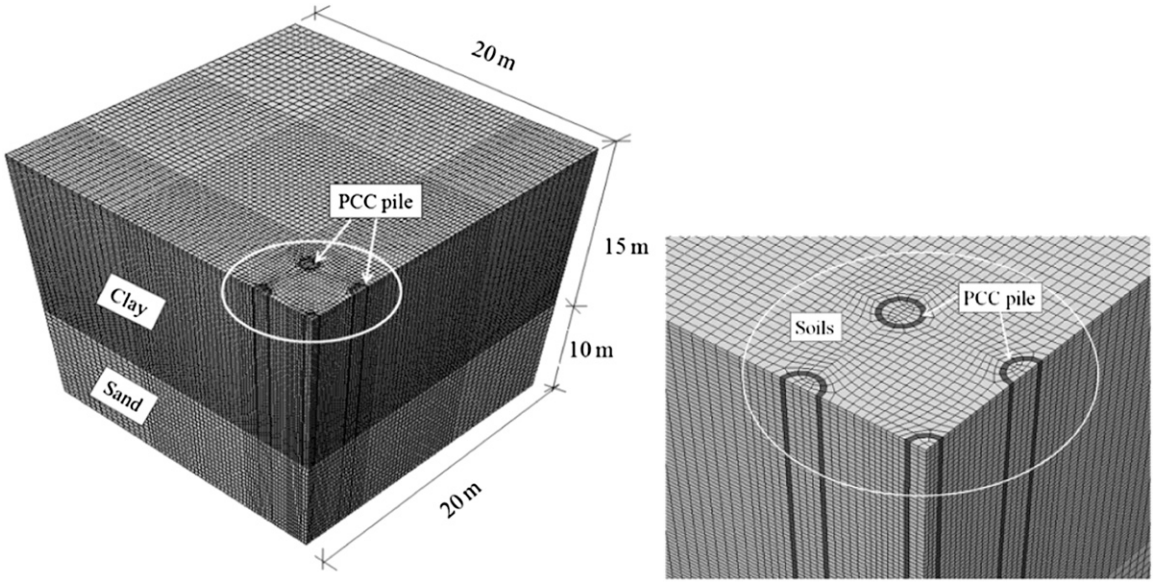

Fig. 8. Geometric meshes and typical finite-element meshes of the 3 × 3 PCC pile group without a pile cap (1/4)

Table 2. Parameters of Materials Used in Influence Factor Analysis Numerical Simulation Model

Material	Modulus, E (MPa)	Poisson's ratio, υ	Cohesion, c_{cu} (kPa)	Friction angle, φ_{cu} (°)	Unit weight, γ (kN/m^3)	Lateral coefficient, K_0
Pile	25,000	0.17	—	—	25.00	1.00
Pile cap	30,000	0.17	—	—	25.00	1.00
Cushion	30	0.30	5.00	35.00	22.00	0.50
Soil	10	0.30	20.00	20.00	18.00	0.65

Table 3. Stratified Soil Parameters Input Data for *LPILE* Analysis

Materials	Thickness (m)	Effective weight, γ' (kN/m^3)	Lateral coefficient, K_0	Consolidated undrained shear test		Undrained confined strength, S_u (kPa)
				Cohesion, c_{cu} (kPa)	Friction angle, φ_{cu} (°)	
Soft clay	2.0	4.70	0.55	24.00	27.00	26.63
Soft clay	1.5	4.70	0.55	24.00	27.00	27.62
Sand	2.5	5.19	0.38	15.00	38.00	22.32
Sand	0.5	5.19	0.38	15.00	38.00	24.63

that of the drilled shaft. Uniform surface friction applied at the pile head through the cushion layer has a relationship with the pile gross section area, which causes the deflection and bending moment of the PCC pile to be larger than those of the drilled shaft.

Influence Analysis with/without Pile Cap

The bending moments of a single PCC pile along the pile with or without a pile cap are shown in Fig. 13. The maximum positive bending moment of the PCC pile with a pile cap is 117.4 kN·m (86.594 ft·kips) at 7 m (22.966 ft) below the pile top. The maximum bending moment of the PCC pile without a pile cap is 202.1 kN·m (149.069 ft·kips), and it occurs 3 m (9.843 ft) below the pile top. The bending moment of the PCC pile with the pile cap is nearly 58% of that of the PCC pile without the pile cap. In addition, when the pile has a pile cap, the negative bending moment of −606.4 kN·m (−447.281 ft·kips) is developed at the pile top.

When pile spacing equals 1.95 m (6.398 ft) (three times the circular pile diameter D_0) and pile top deflection equals 10 mm (0.394 in.), the comparison of lateral bearing capacity and group efficiency of the 3 × 3 PCC pile and drilled shaft are shown in Table 6. Pile group efficiency η is defined as the group lateral bearing capacity Q_g, divided by the sum of the individually lateral bearing capacities Q_s (n roots). The equation is as follows:

$$\eta = \frac{Q_g}{nQ_s} \tag{1}$$

The results show that the lateral bearing capacity of the PCC pile is larger than that of a drilled shaft with the same concrete volume. The bearing capacity of a single PCC pile is nearly 1.5 times that of a drilled shaft; the bearing capacity of the 3 × 3 PCC pile group is nearly 1.3 times that of a drilled shaft. The bearing capacities of a single PCC pile and 3 × 3 PCC pile group with a pile cap are nearly 1.9 times and 1.7 times greater compared with piles without a pile cap, respectively. Similar results are obtained for the drilled shaft. The pile group efficiency of the PCC pile is smaller than that of the drilled shaft. This is because that pile spacing is three times the diameter for a drilled shaft with 1.95-m (6.398-ft) pile spacing, while the pile spacing is only two times the diameter for the PCC pile.

J. Perform. Constr. Facil. 2013.27:191-202.

Influence Analysis of Pile Spacing

Take one condition for example (3×1 pile groups without a cushion layer). The comparative curves of longitudinal pile group efficiency versus pile spacing are shown in Fig. 14. Fig. 14 shows that the longitudinal group efficiency is increased with increasing the pile spacing. This is because the pile-pile interaction is improved by

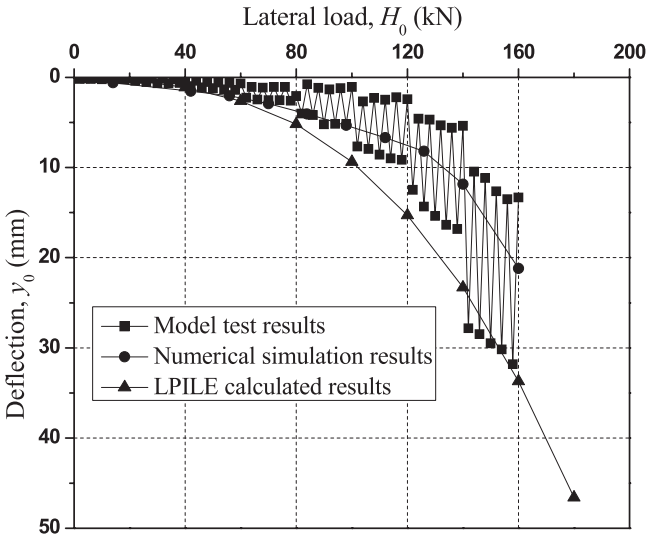

Fig. 9. Comparative curves of the numerical simulation pile top lateral load versus the deflection with that of the *LPILE* calculation and model test results

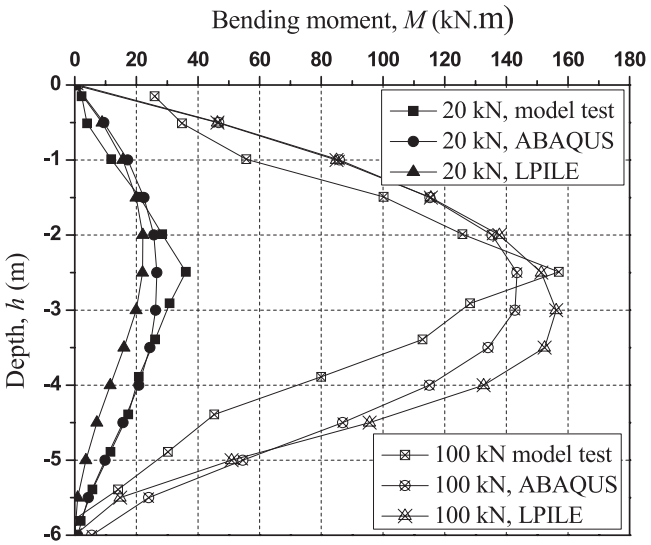

Fig. 10. Comparative curves of numerical simulation bending moment distributions along the pile with those of the *LPILE* calculation and model test results

Table 5. Influence Factors Analysis Conditions

Influence factors	Values				
Vertical load (kPa)	50.0	100.0	200.0	—	—
Cushion thickness (mm)	100.0	200.0	300.0	—	—
Replacement rate (percentage)	3.7	2.1	1.3	—	—
Pile number (roots)	2.0	3.0	4.0	5.0	6.0

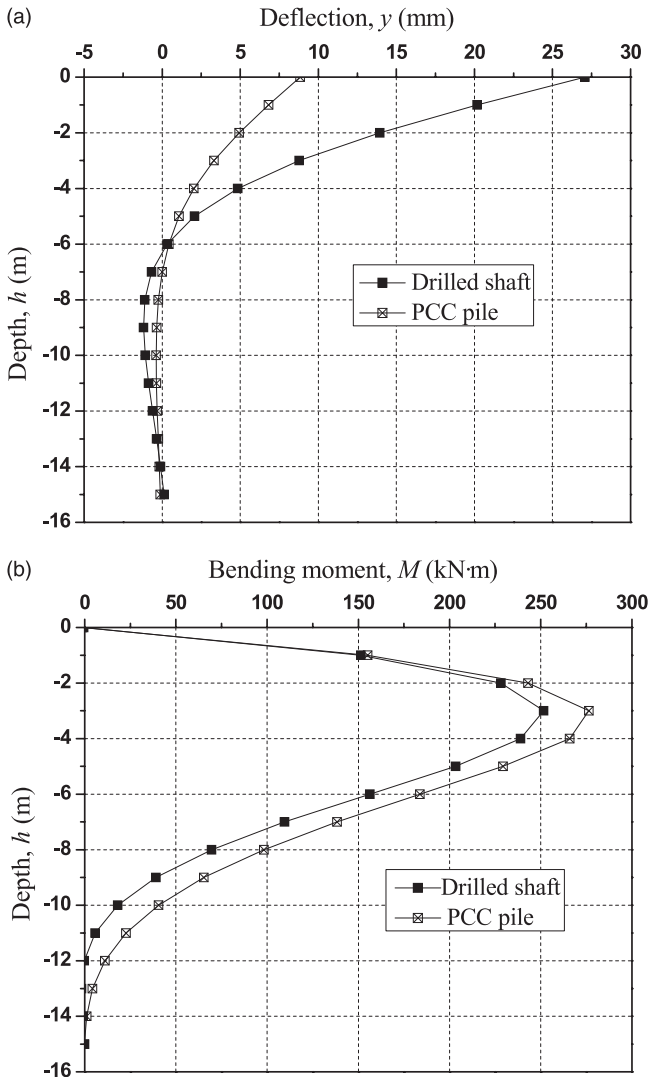

Fig. 11. Comparative curves showing distributions of the deflection and the bending moment along the pile without a cushion layer (lateral load = 200 kN [44.964 kips], vertical load = 0 kPa): (a) deflection; (b) bending moment

Table 4. Comparative Analysis Conditions of Cushion Layer, Pile Cap, and Pile Spacing

	Cushion (mm)		Pile cap (m)		Pile spacing (m)	
Conditions	Cast-in-place concrete pipe pile	Drilled shaft	Cast-in-place concrete pipe pile	Drilled shaft	Cast-in-place concrete pipe pile	Drilled shaft
With	200	200	$4 \times 4 \times 0.4$	$4 \times 4 \times 0.4$	$2–16D_0$	$2–16D_0$
Without	None	None	None	None	None	None

Note: D_0 is the diameter of the drilled shaft, which has the same concrete volume as the cast-in-place concrete pipe pile.

J. Perform. Constr. Facil. 2013.27:191-202.

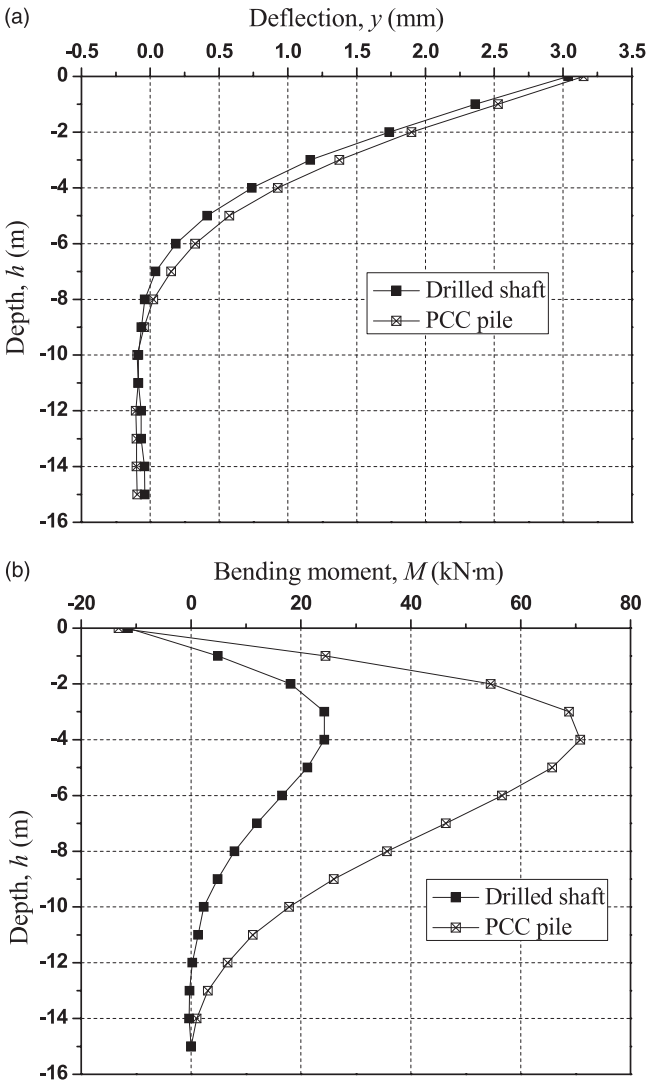

Fig. 12. Comparative curves showing distributions of the deflection and the bending moment along the pile with a cushion layer [lateral load = 125 kPa (18.142 psi), vertical load = 100 kPa (14.514 psi)]: (a) deflection; (b) bending moment

increasing pile numbers. The group efficiency of the PCC pile is smaller than that of the drilled shaft at the same pile spacing. Also, the group efficiency of the pile with a pile cap is smaller than that of the pile without a pile cap.

Influence Factors Analysis

Influence Analysis of Vertical Loads

Fig. 15 shows the distribution of deflection and the bending moment of a PCC pile under different vertical loads and uniform lateral loads (125 kPa [18.142 psi]). The results are similar. The deflection and bending moment values decrease with increasing vertical load. Fig. 15(a) shows that pile deflections are changed from positive to negative 8 m below the pile top. Fig. 15(b) shows that the maximum values of the bending moment are developed 4 m (13.123 ft) below the pile top, and are 73.5 kN·m (54.214 ft·kips), 71.0 kN·m (52.370 ft·kips), and 63.9 kN·m (47.133 ft·kips). A small negative bending moment occurs at the pile top because of the cushion effect.

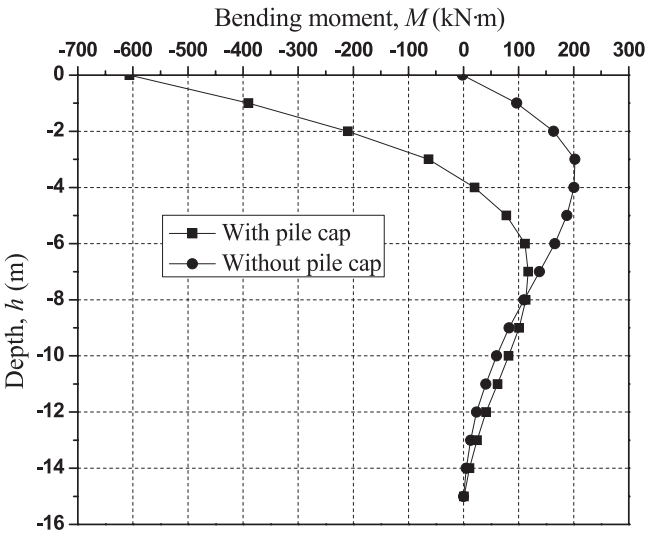

Fig. 13. Comparative curves showing the bending moment of the PCC pile along the pile with or without a pile cap

Table 6. Comparison on Lateral Bearing Capacity and Group Efficiency of 3 × 3 Cast-in-Place Concrete Pipe Pile and Drilled Shaft [Pile Spacing = 1.95 m (6.398 ft), Pile Top Deflection = 10 mm (0.394 in.)]

	Bearing capacity of single pile (kN)		Bearing capacity of pile group (kN)		Pile group effect (percentage)	
Conditions	Cast-in-place concrete pipe pile	Drilled shaft	Cast-in-place concrete pipe pile	Drilled shaft	Cast-in-place concrete pipe pile	Drilled shaft
With pile cap	249.2	163.6	806.4	613.8	36	42
Without pile cap	131.4	85.9	459.0	359.1	39	46

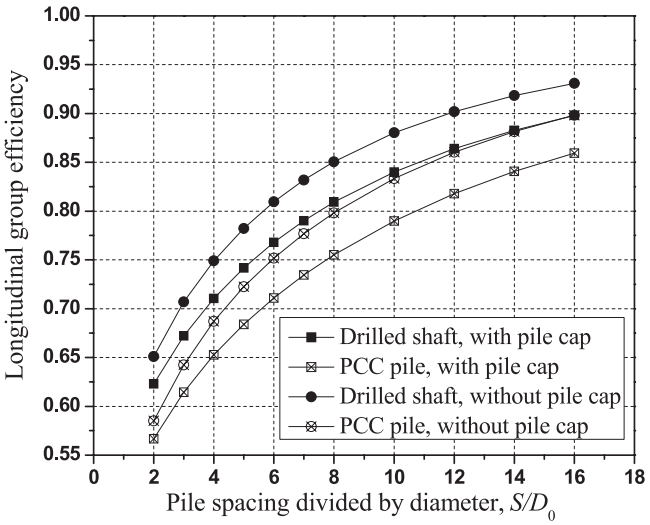

Fig. 14. Comparative curves showing the longitudinal pile group efficiency versus the pile spacing in 3 × 1 row pile groups with or without a pile cap

J. Perform. Constr. Facil. 2013.27:191-202.

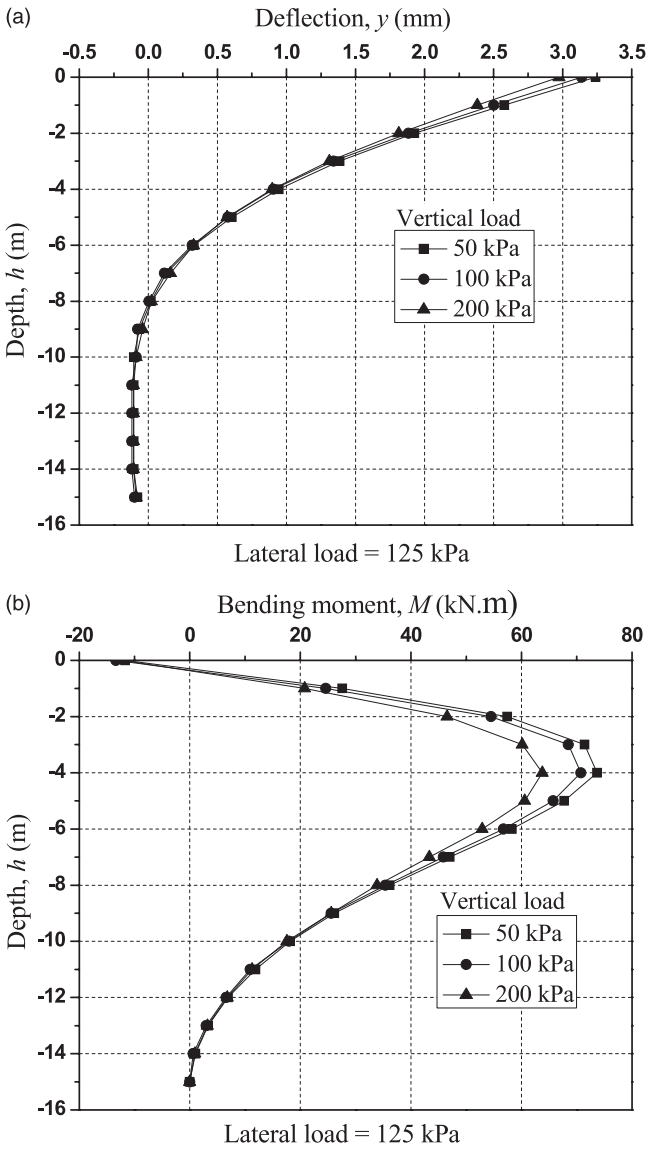

Fig. 15. Comparative curves showing distributions of the deflection and the bending moment along the PCC pile depth under different vertical loads through the cushion soil layer: (a) deflection; (b) bending moment

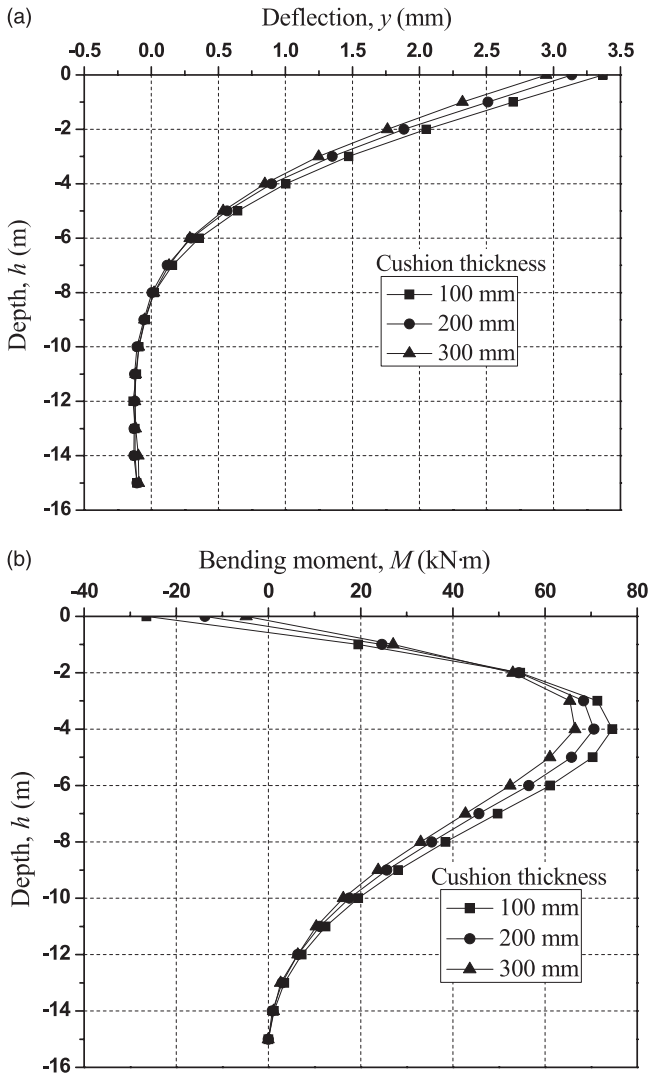

Fig. 16. Comparative curves showing distributions of the deflection and the bending moment along the PCC pile depth under the vertical load influenced by cushion thickness: (a) deflection; (b) bending moment

Influence Analysis of Cushion Thickness

Fig. 16 shows the distribution of deflection and bending moment of a PCC pile with different cushion thickness under lateral loads and uniform vertical loads. The results are similar. The values decrease with an increase in cushion thickness. Fig. 16(a) shows that the top deflections of the PCC pile are 3.4 mm (0.134 in.), 3.2 mm (0.126 in.), and 2.9 mm (0.114 in.). Fig. 16(b) shows that the maximum values of the bending moment are developed at 4 m (13.123 ft) below the pile top, and are 74.8 kN·m (55.172 ft·kips), 71.0 kN·m (52.370 ft·kips), and 66.6 kN·m (49.124 ft·kips). The negative bending moment occurs at the pile top caused by the cushion effect, and the values increase with decreasing cushion thickness.

Influence Analysis of Replacement Rate

The replacement rate is defined as the pile areas divided by the soil areas under one unit loads. The replacement rate is varied by using different pile cap sizes. Three different replacement rates with 1.3, 2.1, and 3.7% are related to 3×3 m (9.843×9.843 ft), 4×4 m (13.123×13.123 ft), and 5×5 m (16.404×16.404 ft) (length × width) pile cap sizes, respectively. When the PCC pile is under a specific lateral load and vertical load, the distributions of the deflection and bending moment of the PCC pile are changed with replacement rates. Fig. 17 shows these relationships. The deflection and bending moment values decrease with the replacement rate increasing. Negative bending moments located at the pile top increase with the decreasing of the replacement rate.

Influence Analysis of the Pile Numbers

The effects of the pile numbers on the PCC pile group efficiencies under $3D_0$ and $6D_0$ pile spacing are shown in Figs. 18(a and b), respectively. Fig. 18 shows that the pile group efficiencies decrease with the increasing of pile numbers. This is because the pile-pile interaction improves with the increasing of pile numbers. At the same time, the longitudinal group efficiencies of the PCC piles are smaller than the transverse group efficiencies. Moreover, the group efficiencies of the pile with a pile cap are smaller than those of the pile without a pile cap.

J. Perform. Constr. Facil. 2013.27:191-202.

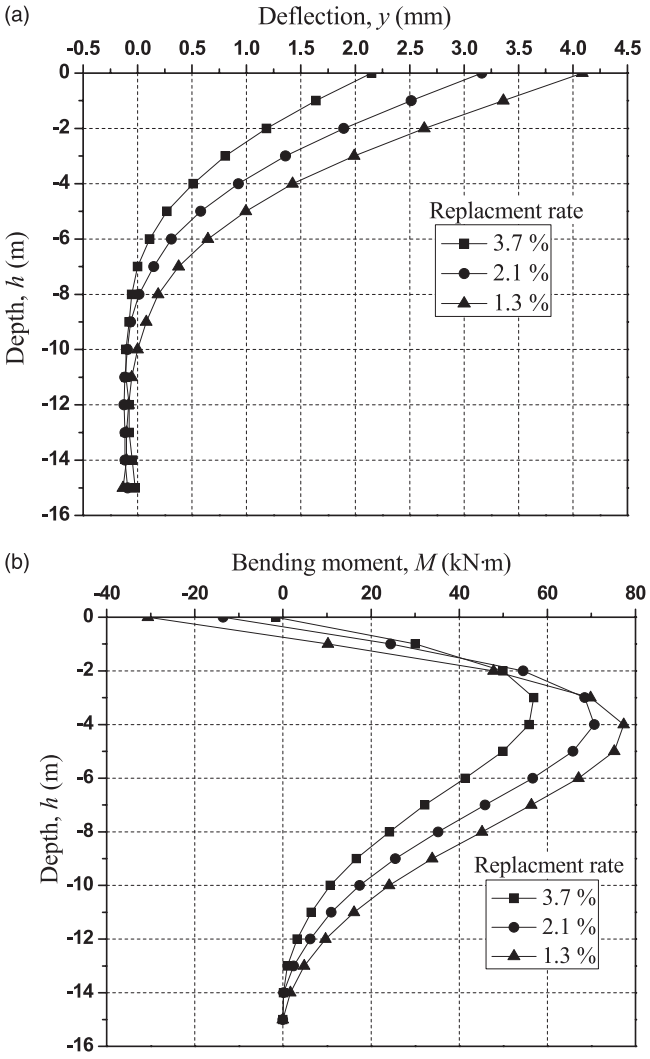

Fig. 17. Comparative curves showing distributions of the deflection and the bending moment along the PCC pile depth under the vertical load influenced by the replacement rate: (a) deflection; (b) bending moment

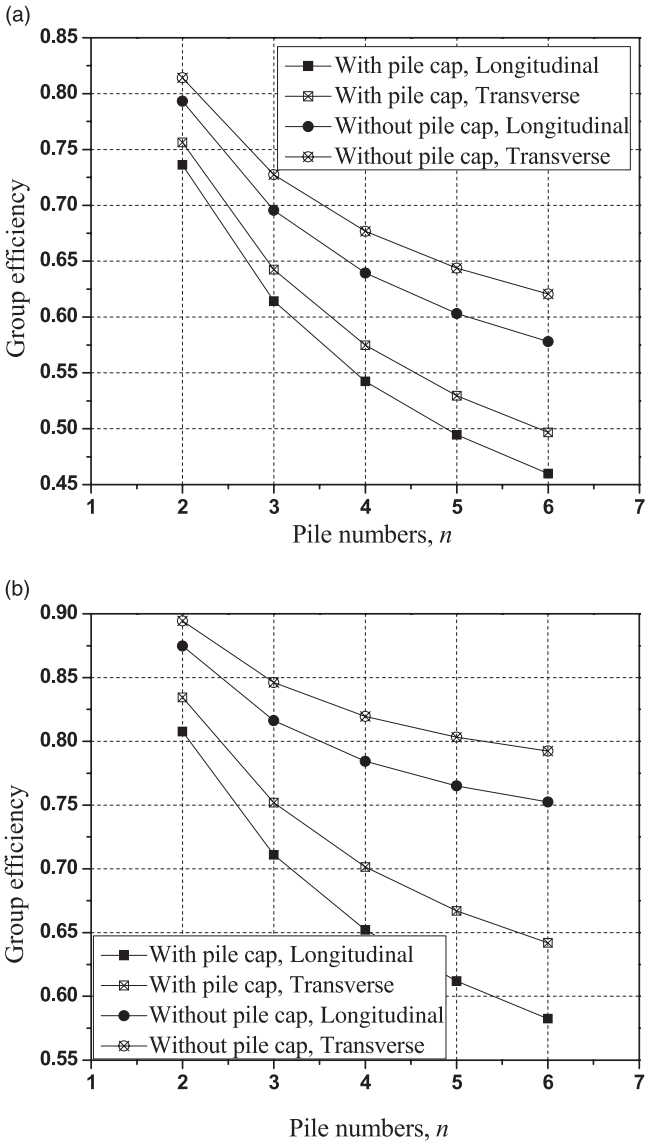

Fig. 18. Comparative curves of pile group efficiency versus pile numbers for the PCC piles: (a) $S = 3D_0$; (b) $S = 6D_0$

Conclusions

The PCC pile or PCC pile-supported embankment under lateral load must be considered in engineering design and construction. Based on the comparative analysis of the PCC pile and the drilled shaft under lateral load, and the influence factors analysis of the PCC pile, the following major conclusions may be drawn from these results.

1. PCC piles under lateral load can be calculated by *p-y* curves developed for the conventional drilled shaft and the modified pile modulus using *LPILE* software, which means that the PCC pile under the lateral load has similar performance with that of a drilled shaft with the same outer diameter. On the other hand, the concrete volume can be reduced using the PCC pile. Large-scale model test results show that the lateral load versus deflection, bending moment distributions along the pile, and *p-y* curves of the PCC pile are similar to those of a drilled shaft. Using *LPILE* software to calculate the model PCC pile was reported by using the modified pile modulus. PCC piles under lateral load can be calculated by the *p-y* curves method, which was developed for the drilled shaft, through comparative analysis of *LPILE* calculated results with those of model test results.
2. When the PCC pile is used for embankment support, the PCC pile-supported embankment is more cost effective than conventional pile-supported embankment. Compared with a conventional drilled shaft, the lateral bearing capacity of the PCC pile can be improved under the same conditions. The lateral bearing capacity of a single PCC pile and pile groups is larger than that of a drilled shaft with the same concrete volume. The deflections of the PCC pile used in the embankment under lateral load decrease with increasing vertical load, increasing cushion thickness, increasing replacement rate, and increasing pile numbers.

Acknowledgments

We acknowledge financial support from the National Natural Science Foundation of China (Grant Nos. 51008116 and 51278170), the National Science Joint High Speed Railway Foundation of China

J. Perform. Constr. Facil. 2013.27:191-202.

(No. U1134207), and the 111 Project (No. B13024). We gratefully acknowledge Dr. Jian-Wei Zhang and Master Xue-Jun Tao for their contributions to the model tests. Finally, Kenneth L. Carper of Washington State University, the three anonymous reviewers, and the editor are sincerely appreciated for their great comments and suggestions, which substantially improved the presentation of this paper.

References

ABAQUS [Computer software]. Pawtucket, RI, Hibbitt, Karlsson & Sorensen, Inc.

American Petroleum Institute. (1993). "Recommended practice for planning designing and constructing fixed offshore platforms—Working stress design." *API RP2A-WSD*, American Petroleum Institute, Washington, DC.

Chen, R. P., Xu, Z. Z., Chen, Y. M., Ling, D. S., and Zhu, B. (2010). "Field tests on pile-supported embankments over soft ground." *J. Geotech. Geoenviron. Eng.*, 136(6), 777–785.

China Academy of Building Research. (2008). "Code for techniques of pile foundation work." *JGJ94-2008*, China Architecture and Building Press, Beijing.

Han, J., and Akins, K. (2002). "Use of geogrid-reinforced and pile supported earth structures." *Proc., Deep Found. 2002: An Int. Perspect. Theor. Design Const. Perform.*, ASCE, Reston, VA, 668–679.

Han, J., and Gabr, M. A. (2002). "Numerical analysis of geosynthetic reinforced and pile-supported Earth platforms over soft soil." *J. Geotech. Geoenviron. Eng.*, 128(1), 44–53.

Jones, C. J. F. P., Lawson, C. R., and Ayres, D. J. (1990). "Geotextile reinforced piled embankments." *Proc., 4th Int. Conf. Geotext. Geomemb. Relat. Prod.*, Balkema, Rotterdam, Netherlands, 155–160.

Lin, K. Q., and Wong, I. H. (1999). "Use of deep cement mixing to reduce settlements at bridge approaches." *J. Geotech. Geoenviron. Eng.*, 125(4), 309–320.

Liu, H. L., Chu, J., and Deng, A. (2009). "Use of large-diameter, cast-in situ concrete pipe piles for embankment over soft clay." *Can. Geotech. J.*, 46(8), 915–927.

Liu, H. L., Ng, C. W. W., and Fei, K. (2007). "Performance of a geogrid-reinforced and pile-supported highway embankment over soft clay: Case study." *J. Geotech. Geoenviron. Eng.*, 133(12), 1483–1493.

Ma, Z. T., Liu, H. L., Zhang, T., and Fei, K. (2006). "Behaviors of PCC pile under lateral loading test." *Rock Soil Mech.*, 27(Supp. 1), 818–821.

Matlock, H. (1970). "Correlations for design of laterally loaded piles in soft clay." *Proc., 2nd Annual Offshore Technology Conf., Paper No. OTC 1204*, Houston, 577–594.

Reese, L. C., Cox, W. R., and Koop, F. D. (1974). "Analysis of laterally loaded piles in sand." *Proc., 6th Offshore Technology Conf.,* Houston, 473–483.

Reese, L. C., Wang, S. T., Isenhower, W. M., Arrellaga, J. A., and Hendrix, J. (2004). *User's manual of LPILE plus 5.0 for Windows*, Ensoft, Inc., Austin, TX.

Wang, S. T., and Reese, L. C. (1993). "COM624P—Laterally loaded pile analysis program for the microcomputer." *Publication No. FHWA-SA-91-048,* Federal Highway Administration, Austin.

Xu, X. T., Liu, H. L., and Lehane, B. M. (2006). "Pipe pile installation effects in soft clay." *Proc., Instit. Civil Eng. Geotech. Eng.*, 159(4), 285–296.

Zhu, X. R., Zhu, M. S., and Wang, J. C. (2006). "Experimental analysis of bearing capacity of cast-in-place tubular pile." *Rock Soil Mech.*, 27(10), 1749–1753.